Journal of Anatomy

J. Anat. (2010) **217**, pp588–596 doi: 10.1111/j.1469-7580.2010.01297.x

Aortic arch morphometry in living humans

Stefanos Demertzis,[1,2] Samuel Hurni,[2] Mario Stalder,[2] Brigitta Gahl,[2] Gudrun Herrmann[3] and Jos Van den Berg[4]

[1]*Department of Cardiac Surgery, Cardiocentro Ticino, Lugano, Switzerland*
[2]*Department of Cardiovascular Surgery, Inselspital, Bern University Hospital, Bern, Switzerland*
[3]*Institute of Anatomy, University Bern, Bern, Switzerland*
[4]*Service of Interventional Radiology, Ospedale Regionale di Lugano, sede Civico, Lugano, Switzerland*

Abstract

Anatomical features of the aortic arch such as its steepness, the take-off angles and the distances between its supra-aortic branches can influence the feasibility and difficulty of interventional and/or surgical maneuvers. These anatomical characteristics were assessed by means of 3D multiplanar reconstruction of thoracic angio-computed tomography scans of 92 living patients (79 males, 13 females, mean age 69.4 ± 9.9 years) carried out for various indications (gross pathology of the thoracic aorta excluded). There was a significant variation of all measured parameters between the subjects – a standard aortic arch (i.e. with all measured parameters within 2 SD) does not seem to exist. There were no significant differences between genders but some of the parameters correlated significantly to age.

Key words anatomy; aortic arch; computed tomography scan; human; morphometry; supra-aortic arteries.

Introduction

The aortic arch and supra-aortic branches are important anatomical structures for both surgeons and interventionalists. Aneurysms or dissections of the aortic arch need to be treated with complex surgical procedures such as deep hypothermic circulatory arrest and selective antegrade cerebral perfusion. These procedures evolved to enable replacement of the aortic arch and reconstruction of its continuity to the aorta and supra-aortic arteries with less risk of ischemic and/or embolic cerebral damage. General and neurological morbidity, however, are still significant especially in elderly patients and/or in patients already burdened with significant co-morbidities. This is the motivation to find less invasive treatment options such as aneurysm exclusion with endovascular stent grafts.

Interventionalists have to cross the aortic arch to access the supra-aortic arteries with catheters. Intravascular procedures, such as percutaneous angioplasty and stenting of the internal carotid arteries or other supra-aortic arteries and occlusion of intracerebral aneurysms with coils, are well-accepted treatment options and have good acute and long-term results.

Correspondence
Stefanos Demertzis, Department of Cardiac Surgery, Cardiocentro Ticino, Via Tesserete 48, CH-6900 Lugano, Switzerland.
T: +41 91 8053144; F: +41 91 8053148; E: demertzis@cardiocentro.org

Accepted for publication *6 August 2010*

Knowledge of morphometric data of the aortic arch can be of help for conceiving, designing and optimizing all types of diagnostic and/or therapeutic interventions involving the aortic arch. In any individual case, physicians have the opportunity to assess individual anatomy and plan the procedure accordingly. However, for developing new procedures or optimizing existent ones, knowledge of the distribution, regularity or irregularity and typology of several anatomical characteristics is crucial.

Interventional and hybrid approaches for the treatment of aortic arch aneurysms are novel emerging treatment strategies for diseases associated with significant morbidity and mortality. Knowledge of the morphometric anatomical characteristics of the aortic arch and its supra-aortic branches could be helpful for all those involved in this young but rapidly developing and complex field.

Materials and methods

Anonymized thoracic computed tomography (CT) angiography scans from patients undergoing diagnostic evaluation for various indications served as a basis for this work. Patients with thoracic aortic pathology (e.g. aneurysms) were excluded. The CT scans were performed using either a 16-slice Sensation (Siemens Medical Solutions, Forchheim, Germany) or a 64-slice LightSpeed VCT (GE Healthcare, Waukesha, WI, USA) multidetector scanner. The technical characteristics of the scanning procedure were as follows (for the 16-slice and 64-slice scanners, respectively): collimation 0.75/0.63 mm, pitch 0.25/0.24 mm, reconstruction slice thickness 1.0/0.63 mm, increment 1.0/0.63 mm. In each case, scanning was carried out using 120 mL of contrast medium with an iodine content of > 300 mg mL^{-1} at a flow rate of 4 mL s^{-1}.

Further processing was performed with the DICOM imaging software OsiriX (version 3.6.1; http://www.osirix-viewer.com/) on computers running Mac OS 10.6.3.

Processing was based on 3D multiplanar reconstruction. Multiplanar reconstruction was initiated in the axial view in the sagittal and coronal plane (Fig. 1). Subsequently, reconstruction planes were oriented along the long axis of the aortic arch at the origin of each supra-aortic artery. With this orientation the parasagittal plane yields a frontal 'stretched-out' 2D view of the aortic arch (Fig. 1). The take-off angles of all supra-aortic arteries were measured individually in all described planes. In the parasagittal plane, the angles were measured with respect to the horizontal plane (anatomical view), as well as with respect to a line drawn tangentially to the convexity of the aortic arch at the origin of each vessel (long axis – surgical view). The distances between the origins of the supra-aortic arteries were also measured in this projection.

The aortic arch is described in three ways: (i) by the aortic arch angle defined as the angle between a line connecting the highest point of the aortic arch and a mid-luminar point of the ascending and descending aorta at the height of the bifurcation of the pulmonary trunk in the parasagittal plane (Fig. 2D) (Agnoletti et al. 2008); (ii) by the angle between the horizontal plane and the long axis of the three arch segments defined by the origins of the supra-aortic arteries in the axial view (curvature 1, curvature 2 and curvature 3, respectively, Fig. 2); and (iii) by the aortic arch type (I, II or III, Fig. 3) using as criterion the vertical distance from the origin of the brachiocephalic trunk (BT) to the top of the arch in the parasagittal 'stretched-out' projection. This distance is < 1 diameter of the left common carotid artery (LCA) in a type I arch, between 1 and 2 diameters in a type II arch, and > 2 diameters in a type III arch (Madhwal et al. 2008).

Statistical analysis focused on descriptive statistics, differences between genders and arch types, as well as correlations with age and was performed with the SPSS Advanced Statistics software package (version 17; SPSS, Inc., Chicago, IL, USA). Differences between genders and aortic arch type were tested with chi-squared tests, differences of means of the measured parameters between genders were tested with the Mann–Whitney test, and differences of means between the aortic arch types were tested with the Kruskal–Wallis test. Correlations were expressed with Pearson's correlation coefficient and tested two-sided. The *P*-level for statistical significance was 0.05.

The measuring of angles and distances was performed by two of the authors (S.H. and S.D.). Inter-rater variability was tested for a trend with paired Student's *t*-test and by means of Bland–Altman plots for agreement.

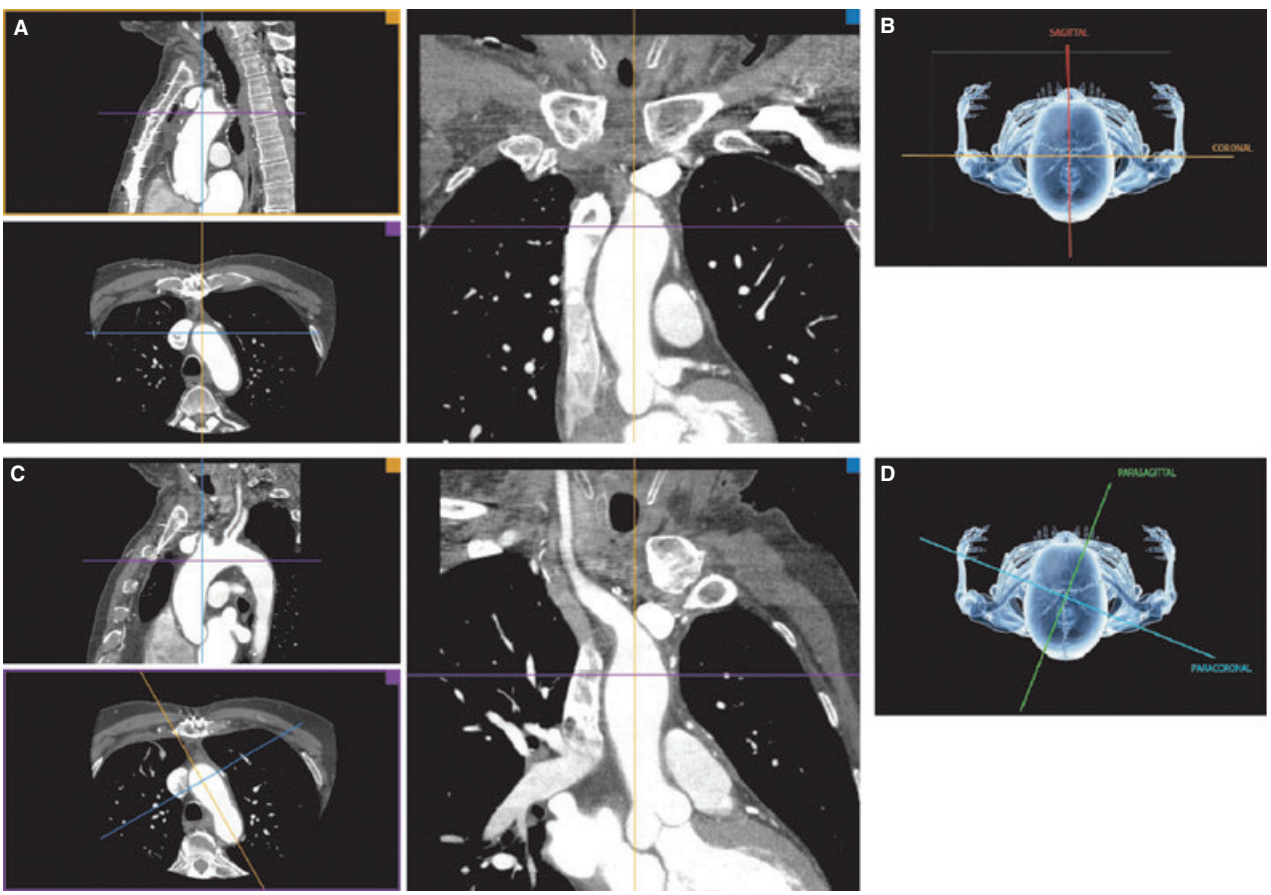

Fig. 1 Representation of the sagittal, coronal, parasagittal (PS) and paracoronal (PC) multiplanar reconstruction (MPR) planes. (A and C) Bottom left: MPR planes in the axial view; top left: sagittal and PS planes; right: coronal and PC views. (B and D) Graphical representation of the respective planes.

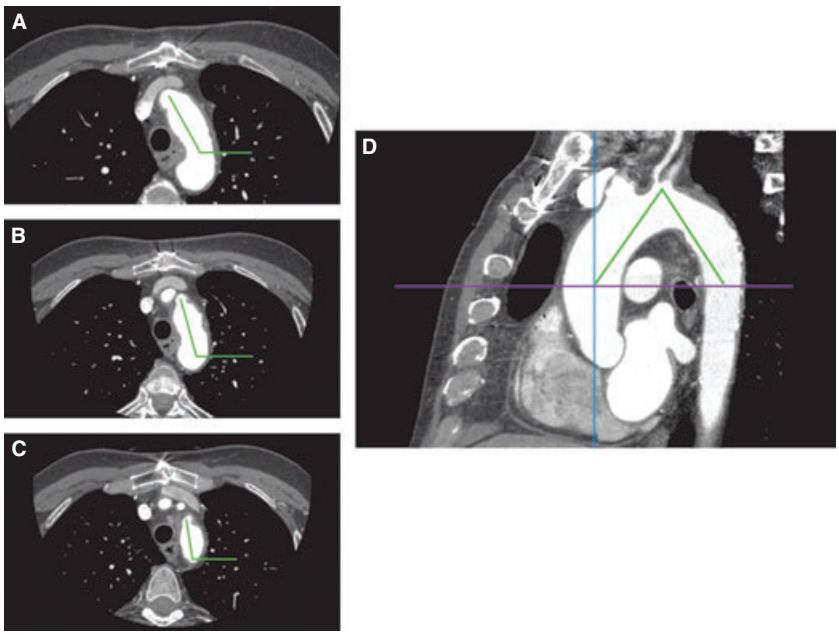

Fig. 2 Aortic arch curvature of segments 1, 2 and 3 (A–C) and aortic arch angulation (D). In D the horizontal axis is placed at the height of the bifurcation of the pulmonary trunk.

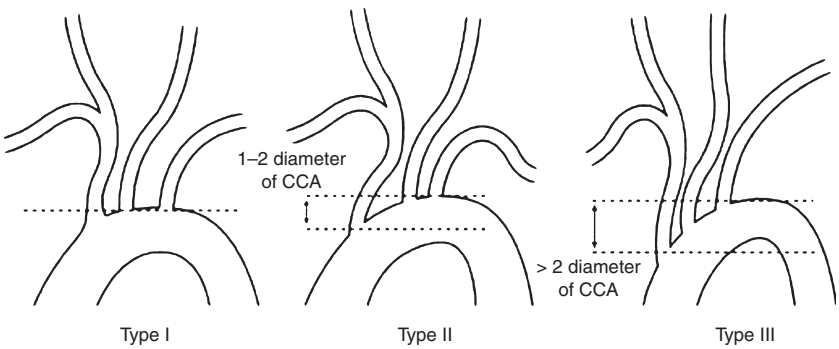

Fig. 3 Aortic arch types [reprinted from Madhwal et al. (2008) with permission from HMP Communications]. CCA: left common carotid artery.

Naming of the measured angles was composed as follows: the English abbreviation of the respective structure, underscore, the visualization plane, underscore and the reference for the angle measurement. For example, 'BT_PS_LA' stands for BT in the parasagittal plane, angle measured with reference to the long axis of the aortic arch. The distances were named by the two supra-aortic vessels defining the distance separated by an underscore. The supra-aortic vessels were abbreviated as follows: brachiocephalic trunk (BT), left common carotid artery (LCA) and left subclavian artery (LSA). The anatomical planes were: sagittal (S), coronal (C), parasagittal (PS) and paracoronal (PC), and the references for the angle measurements were: horizontal (H) and long axis of the aortic arch (LA).

Results

Normal anatomy was encountered in 82 patients. Among the remaining 10 patients, there were eight with a common origin of the right and left common carotid artery and in two instances there were separate origins of the right subclavian artery directly from the aortic arch.

In the axial view, the aortic arch showed different inclinations in its helicoidal curve around the structures of the superior mediastinum with the angles becoming increasingly more steep. The first segment (arch 1) between the origins of the BT and the LCA showed an inclination of 126 ± 10° to the horizontal (coronal) plane, the second (arch 2) 114 ± 8° and the third (arch 3) 105 ± 9°, respectively.

The results of all measurements, as well as basic descriptive statistics, are presented in Fig. 4. A statistically significant correlation to age was identified for four angles with regard to the left carotid artery and LSA, as well as for the distance between the BT and LCA (BT_LCA, $P = 0.047$). The angles correlated to age were: LCA_PS_LA ($P = 0.036$), LSA_S ($P = 0.039$), LSA_PS_LA ($P = 0.03$) and LSA_PS_H ($P = 0.05$). The correlation diagrams are presented in Fig. 5.

A type I aortic arch was identified in 43 (47%), type II in 33 (36%) and type III in 16 (17%) patients. There were

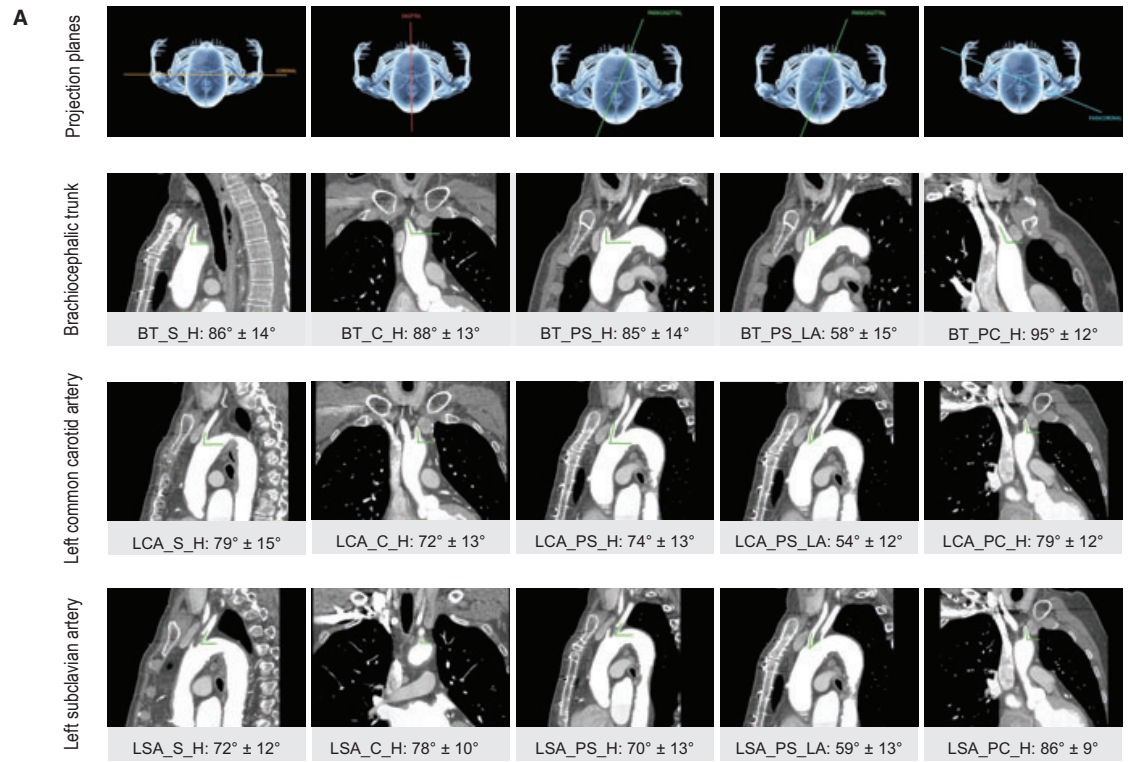

B

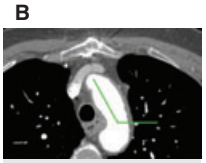
Arch 1: 126° ± 10°

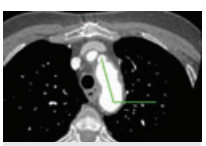
Arch 2: 114° ± 8°


Arch 3: 105° ± 8°

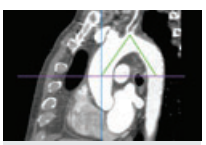
Arch angulation: 62° ± 8°

Angles	*N*	Mean	SD	SEM	95% CI		Minimum	Maximum
					Lower limit	Upper limit		
BT_S_H	92	85.92	14.12	1.47	82.99	88.84	53.90	122.00
BT_C_H	92	87.59	12.99	1.35	84.90	90.28	55.00	118.30
BT_PS_H	92	84.79	13.75	1.43	81.94	87.63	51.60	123.70
BT_PS_LA	92	58.11	14.71	1.53	55.06	61.15	27.30	96.00
BT_PC_H	92	94.68	11.77	1.23	92.25	97.12	60.40	123.20
LCA_S_H	83	78.48	14.65	1.61	75.28	81.68	37.00	130.00
LCA_C_H	83	71.93	12.87	1.41	69.12	74.74	45.00	96.90
LCA_PS_H	83	73.90	13.20	1.45	71.02	76.78	40.30	106.40
LCA_PS_LA	83	54.30	12.37	1.36	51.59	57.00	22.30	82.90
LCA_PC_H	83	78.48	11.49	1.26	75.97	80.99	48.50	104.30
LSA_S_H	92	72.35	11.96	1.25	69.87	74.82	47.20	100.60
LSA_C_H	92	78.32	9.72	1.01	76.31	80.33	54.00	97.80
LSA_PS_H	92	70.16	12.52	1.31	67.57	72.75	48.50	100.50
LSA_PS_LA	92	59.34	13.04	1.36	56.64	62.04	36.20	90.30
LSA_PC_H	92	85.93	9.33	0.97	84.00	87.86	64.30	112.60
Curvature 1	92	125.78	10.38	1.08	123.64	127.93	106.40	157.20
Curvature 2	83	114.37	7.67	0.84	112.70	116.05	93.80	131.30
Curvature 3	92	105.30	9.22	0.96	103.39	107.21	77.80	126.70
Arch angulation	91	61.89	7.64	0.80	60.30	63.48	42.60	80.30
Distances (cm)								
BT_LCA	83	1.31	0.34	0.04	1.24	1.39	0.70	2.40
LCA_LSA	83	1.88	0.42	0.05	1.78	1.97	1.10	3.30
BT_LSA	9	2.33	0.48	0.16	1.96	2.70	1.60	3.00

Fig. 4 Graphical representation of all results. (A) First row indicates the respective projection planes and the three lower rows illustrate and group the means ± 1 SD of take-off angles of the three supra-aortic arteries in the respective projections. Supra-aortic arteries: BT, brachiocephalic trunk; LCA, left common carotid artery; LSA, left subclavian artery. Anatomical planes: S, sagittal; C, coronal; PS, parasagittal; PC, paracoronal. References for the angle measurements: H, horizontal; LA, long axis of the aortic arch. (B) Photographs illustrate the means ± 1 SD of the inclination of the three aortic arch segments and the aortic arch angulation. The embedded table summarizes the descriptive statistics of all measured parameters. CI, confidence interval.

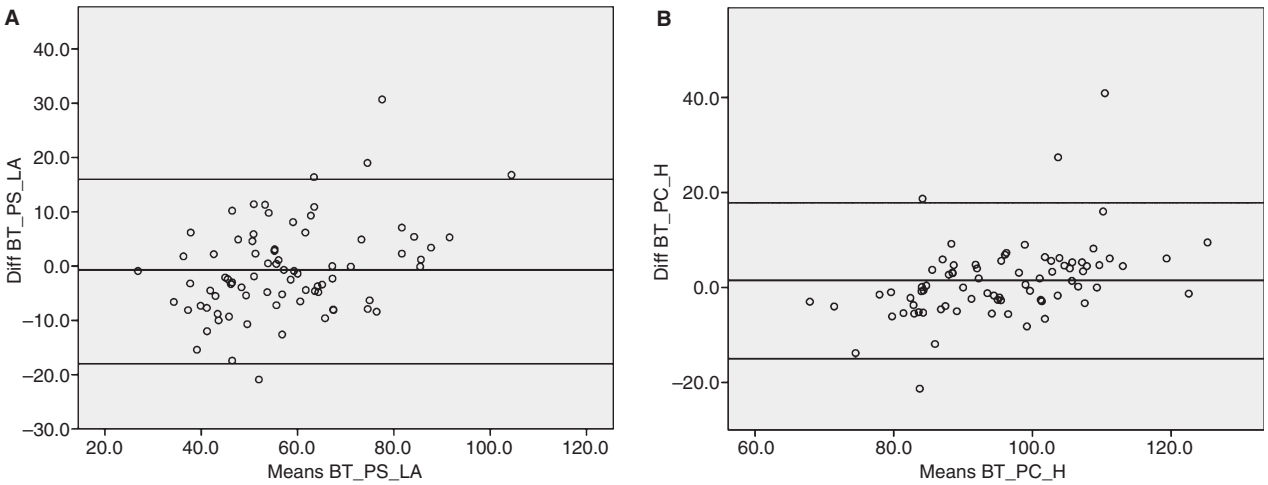

Fig. 5 Bland-Altman plots for assessment of inter-rater variability. Measurements of the parameters BT_PS_LA (A) and BT_PC_H (B) are shown.

several statistically significant differences in the measured parameters between the three arch types. These results are shown in Table 1. There was no statistically significant difference in the distribution of the aortic arch types between genders (Pearsons's chi-square, $P = 0.225$).

There were no statistically significant differences in all measured angles, distances and arch typology between genders with the exception of the distance between the BT and LCA (135 ± 34 and 109 ± 23 mm in men and women, respectively, $P = 0.011$). The distances in the eight patients with a common origin of the BT and LCA were excluded from this analysis but are presented in Table 1 as the distance between the BT and LSA.

There were no statistically significant differences and thus no systematic deviation between the values measured by the two operators. The Bland–Altman plots for the take-off angle of the BT in the PS projection referred to the LA, as well as the same angle in the PC view, are shown in Fig. 6. As expected, the agreement is not perfect but is still acceptable.

Discussion

Interventional and hybrid approaches for the treatment of aortic arch aneurysms are novel emerging treatment strategies for diseases associated with significant morbidity and mortality. Knowledge of the morphometric anatomical characteristics of the aortic arch and its supra-aortic branches could be helpful for all those involved in this young but rapidly developing and complex field.

Our research was based on angio-CT scans of 92 patients performed for various indications (aortic pathology excluded), hence on living subjects. All measurements and assessments are referred to the main anatomical planes of the human body (sagittal and coronal), as well as to planes, which permit a more functional view of the respective anatomical elements (PS and PC). In addition, the angles are referred not only to the horizontal plane but also to the long axis of the respective segment of the aortic arch, a more functional angle description.

Perhaps the most intriguing result is that a 'standard aortic arch' does not really exist. The database search for patients with all measured characteristics within 2 SD of the calculated mean values yielded only one positive match. This is obviously due to the complex 3D structure of the aortic arch with its helicoidal change of planes from its proximal to distal segments towards the descending aorta; the inclination of the three arch segments in the axial view indicates a curvature around the vertebral column of three different radii with progressive steepness from the first to the third segment.

The configuration of the whole arch in the PS view is of particular interest for catheter access especially of the BT and right common carotid artery, as well as for the feasibility of endovascular stent graft placement up to the origins of the LSA and/or LCA. An arch that is too steep requires difficult maneuvers and, in addition, current endovascular stent grafts cannot adapt to the acute angle inducing stenosis. We convey this information using two parameters: the aortic arch angulation and distribution of aortic arch types.

The aortic arch angulation was proposed by Agnoletti et al. (2008) in angiographic studies. The major reference point is the height of the bifurcation of the pulmonary trunk. Our measurements were carried out in the PS plane. Fine adjustment of the plane orientation was required to get all three reference points (sinotubular junction, 'highest arch point', descending aorta at the height of the bifurcation of the pulmonary trunk) on the same plane. For most of the parameters measured there was an important difference between the minimal and maximal values encountered (43 and 80°, respectively),

Table 1 Comparison of patient age, angles and distances between the three types of aortic arch.

						95% CI		
	Arch type	*n*	Mean	SD	SEM	Lower limit	Upper limit	*P*-value
Age (years)	I	41	67.35	8.66	1.35	64.61	70.08	0.018*
	II	33	68.67	11.57	2.01	64.56	72.77	
	III	18	74.67	7.52	1.77	70.93	78.41	
BT_S (°)	I	41	84.84	13.54	2.11	80.56	89.11	0.769
	II	33	86.17	12.99	2.26	81.57	90.78	
	III	18	87.91	17.63	4.15	79.14	96.67	
BT_C (°)	I	41	87.60	13.98	2.18	83.19	92.01	0.774
	II	33	88.09	12.47	2.17	83.67	92.51	
	III	18	86.66	12.24	2.88	80.57	92.74	
	III	17	88.24	15.98	3.87	80.02	96.45	
BT_PS_H (°)	I	41	83.55	12.89	2.01	79.48	87.62	0.411
	II	33	84.65	14.52	2.53	79.51	89.80	
	III	18	87.84	14.49	3.41	80.64	95.05	
BT_PS_LA (°)	I	41	64.54	13.25	2.07	60.36	68.72	0.000*
	II	33	54.84	13.92	2.42	49.91	59.78	
	III	18	49.44	13.43	3.16	42.76	56.12	
BT_PC_H (°)	I	41	95.18	12.03	1.88	91.38	98.97	0.650
	II	33	95.41	11.31	1.97	91.40	99.42	
	III	18	92.22	12.32	2.90	86.10	98.35	
LCA_C (°)	I	34	67.55	13.51	2.32	62.83	72.26	0.011*
	II	32	72.84	11.49	2.03	68.70	76.99	
	III	17	78.99	11.01	2.67	73.33	84.65	
LCA_S (°)	I	34	71.77	14.19	2.43	66.82	76.72	0.002*
	II	32	80.43	10.75	1.90	76.56	84.31	
	III	17	88.24	15.98	3.87	80.02	96.45	
LCA_PS_H (°)	I	34	66.33	12.42	2.13	62.00	70.66	0.000*
	II	32	76.57	10.18	1.80	72.90	80.24	
	III	17	84.02	11.35	2.75	78.18	89.86	
LCA_PS_LA (°)	I	34	55.89	13.33	2.29	51.24	60.54	0.380
	II	32	53.64	12.16	2.15	49.26	58.03	
	III	17	52.33	11.01	2.67	46.67	57.99	
LCA_PC_H (°)	I	34	75.61	11.56	1.98	71.58	79.64	0.067
	II	32	78.93	12.00	2.12	74.60	83.25	
	III	17	83.39	8.86	2.15	78.83	87.94	
LSA_C (°)	I	41	75.57	9.71	1.52	72.50	78.63	0.006*
	II	33	78.75	9.67	1.68	75.32	82.18	
	III	18	83.79	7.57	1.78	80.02	87.55	
LSA_S (°)	I	41	68.07	10.50	1.64	64.76	71.39	0.005*
	II	33	74.38	12.48	2.17	69.96	78.81	
	III	18	78.35	11.10	2.62	72.83	83.87	
LSA_PS_H (°)	I	41	65.78	9.79	1.53	62.69	68.87	0.003*
	II	33	71.33	14.09	2.45	66.34	76.33	
	III	18	77.97	11.26	2.65	72.37	83.57	
LSA_PS_LA (°)	I	41	64.10	10.65	1.66	60.74	67.46	0.000*
	II	33	58.64	15.15	2.64	53.27	64.02	
	III	18	49.77	7.64	1.80	45.97	53.57	
LSA_PC_H (°)	I	41	85.50	10.18	1.59	82.29	88.72	0.963
	II	33	85.95	8.02	1.40	83.10	88.79	
	III	18	86.89	9.96	2.35	81.93	91.84	
Curvature 1 (°)	I	41	122.73	8.32	1.30	120.10	125.36	0.068
	II	33	127.67	11.41	1.99	123.62	131.71	
	III	18	129.29	11.23	2.65	123.71	134.88	
Curvature 2 (°)	I	34	114.00	8.09	1.39	111.18	116.82	0.928
	II	32	114.59	8.04	1.42	111.69	117.49	
	III	17	114.70	6.38	1.55	111.42	117.98	

Table 1 (Continued).

	Arch type	*n*	Mean	SD	SEM	95% CI		*P*-value
						Lower limit	Upper limit	
Curvature 3 (°)	I	41	106.60	8.29	1.29	103.99	109.22	0.231
	II	33	105.45	10.27	1.79	101.80	109.09	
	III	18	102.07	8.90	2.10	97.65	106.50	
Arch angulation (°)	I	41	65.70	6.59	1.03	63.62	67.78	0.000*
	II	32	60.19	7.02	1.24	57.66	62.73	
	III	18	56.22	6.53	1.54	52.97	59.47	
Distance BT_LCA (cm)	I	34	1.26	0.23	0.04	1.18	1.34	0.686
	II	32	1.34	0.33	0.06	1.22	1.46	
	III	17	1.38	0.50	0.12	1.12	1.63	
Distance LCA_LSA (cm)	I	34	1.77	0.37	0.06	1.64	1.90	0.261
	II	32	1.96	0.39	0.07	1.82	2.10	
	III	17	1.92	0.54	0.13	1.64	2.19	
Distance BT_LSA (cm)	I	7	2.31	0.43	0.16	1.92	2.71	0.177
	II	1	1.80	–	–	–	–	
	III	1	3.00	–	–	–	–	

*Statistical significance at the *P*-value. CI, confidence interval. For the abbreviations of the measured parameters refer to the text.

which points towards a significant variability in the steepness of the aortic arch.

The aortic arch type proposed by Madhwal et al. (2008) gives an additional impression of the steepness of the aortic arch. The type III arch was already correlated to the grade of difficulty of interventional maneuvers for supra-aortic artery access. We found type I to be more frequently represented in our patients (47%) followed by type II (36%).

There was no statistically significant relationship between age, gender and arch type.

A common origin of the BT and LCA (truncus bicaroticus, 'bovine ach') was present in eight of our patients (8.7%), in line with older indications from cadaveric reports for the prevalence of this configuration (De Garis et al. 1933; Layton et al. 2006).

The distances between the origins of the supra-aortic arteries showed important variations, a fact frequently appreciated in surgery, as well as in the angiography suite. The described variation in distance and also in arrangement (not reported) highlights the current need for custom-made devices for the majority of patients. Ingenious solutions to this problem will be required if 'off-the-shelf' stentgraft systems are to be produced in the future.

Measurements of the take-off angles of the supra-aortic arteries on fixated cadavers were reported recently (Shin et al. 2008). In this study the referred angle corresponds to our 'surgical view', i.e. the angle in the PS plane between the first segment of the respective supra-aortic artery and the LA. All three angles reported by Shin et al. (2008) were slightly larger than those measured by us. The fixation process, open preparation of the non-pressurized aortic arch, as well as imprecision in the choice of the correct radiological visualization plane could be possible explanations for this difference.

Age was significantly and positively correlated with the take-off angles of the LCA and LSAs, as well as with the distance between the origins of the BT and LCA. We interprete these results as a natural consequence of the elongation of the whole aorta and aortic arch found with increasing age (Sugawara et al. 2008).

The measurements of angles and distances on CT scans are subject to many operator-driven variations. Projection adjustment, precise placement of the points for the software tools for angle and distance measurement, and accuracy in the choice of the correct axis are some of the factors that account for intra- and interindividual operator variations. We tested the overall agreement of the mean values, a rough criterion, as well as the agreement of the measured values for the same parameter by means of a Bland–Altman plot. For testing, we chose one parameter with a high potential for interoperator variability (the orifice of the BT is wide and the long axis of an arch segment is difficult to draw), the take-off angle of the BT referred to the LA. Notwithstanding the above, interoperator variability was acceptable.

In summary, we present an extensive morphometric analysis of the aortic arch based on angio-CT scans of 92 living humans without gross aortic pathology. Our results could contribute to the continuous effort to improve the treatment and management of aortic arch disease.

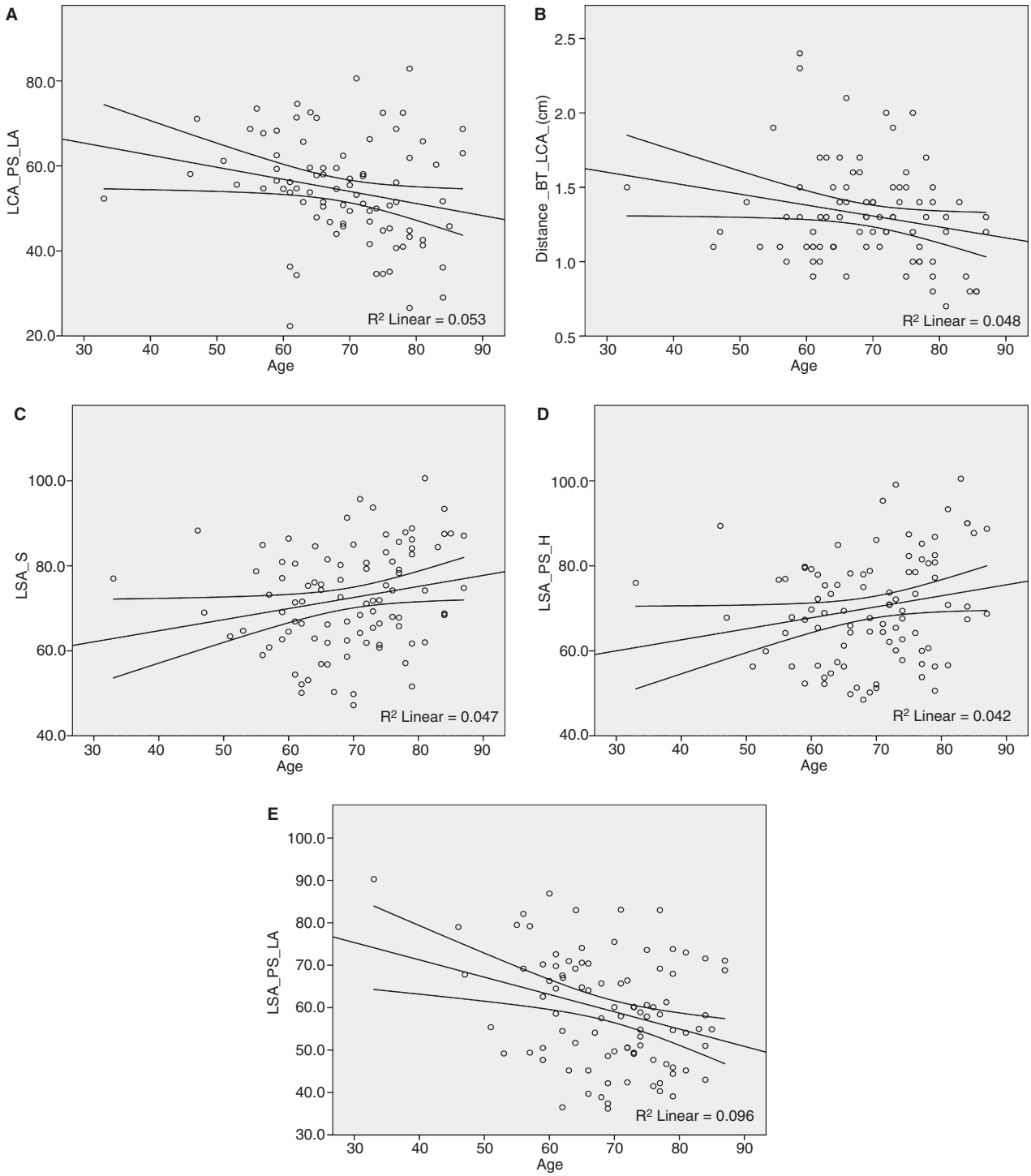

Fig. 6 The statistically significant correlations to age: (A) angle LCA_PS_LA, (B) distance BT_LCA, (C) angle LSA_S, (D) angle LSA_PS_H and (E) LSA_PS_LA (for naming convention please refer to Materials and methods, as well as to the legend of Fig. 4).

References

Agnoletti G, Ou P, Celermajer DS, et al. (2008) Acute angulation of the aortic arch predisposes a patient to ascending aortic dilatation and aortic regurgitation late after the arterial switch operation for transposition of the great arteries. *J Thorac Cardiovasc Surg* **135**, 568–572.

De Garis C, Black I, Riemenschneider E (1933) Patterns of the aortic arch in American White and Negro stocks, with comparative notes on certain other mammals. *J Anat* **67**, 599–618.

Layton KF, Kallmes DF, Cloft HJ, et al. (2006) Bovine aortic arch variant in humans: clarification of a common misnomer. *AJNR Am J Neuroradiol* **27**, 1541–1542.

Madhwal S, Rajagopal V, Bhatt DL, et al. (2008) Predictors of difficult carotid stenting as determined by aortic arch angiography. *J Invasive Cardiol* **20**, 200–204.

Shin I-Y, Chung Y-G, Shin W-H, et al. (2008) A morphometric study on cadaveric aortic arch and its major branches in 25 Korean adults: the perspective of endovascular surgery. *J Korean Neurosurg Soc* **44**, 78–83.

Sugawara J, Hayashi K, Yokoi T, et al. (2008) Age-associated elongation of the ascending aorta in adults. *JACC Cardiovasc Imaging* **1**, 739–748.